

REPORT DOCUMENTATION PAGE				Form Approved OMB NO. 0704-0188	
<p>The public reporting burden for this collection of information is estimated to average 1 hour per response, including the time for reviewing instructions, searching existing data sources, gathering and maintaining the data needed, and completing and reviewing the collection of information. Send comments regarding this burden estimate or any other aspect of this collection of information, including suggestions for reducing this burden, to Washington Headquarters Services, Directorate for Information Operations and Reports, 1215 Jefferson Davis Highway, Suite 1204, Arlington VA, 22202-4302. Respondents should be aware that notwithstanding any other provision of law, no person shall be subject to any penalty for failing to comply with a collection of information if it does not display a currently valid OMB control number.</p> <p>PLEASE DO NOT RETURN YOUR FORM TO THE ABOVE ADDRESS.</p>					
1. REPORT DATE (DD-MM-YYYY) 19-10-2011		2. REPORT TYPE Conference Proceeding		3. DATES COVERED (From - To) -	
4. TITLE AND SUBTITLE Infrared/Terahertz Double Resonance for Chemical Remote Sensing: Signatures and Performance Predictions				5a. CONTRACT NUMBER W911NF-09-1-0428	
				5b. GRANT NUMBER	
				5c. PROGRAM ELEMENT NUMBER 611102	
6. AUTHORS D. J. Phillips , E. A. Tanner , H. O. Everitt, I. R. Medvedev , C. F. Neese , J. Holt, F. C. De Lucia				5d. PROJECT NUMBER	
				5e. TASK NUMBER	
				5f. WORK UNIT NUMBER	
7. PERFORMING ORGANIZATION NAMES AND ADDRESSES Ohio State University Research Foundation Office of Sponsored Programs Ohio State University Research Foundation Columbus, OH 43210 -1063				8. PERFORMING ORGANIZATION REPORT NUMBER	
9. SPONSORING/MONITORING AGENCY NAME(S) AND ADDRESS(ES) U.S. Army Research Office P.O. Box 12211 Research Triangle Park, NC 27709-2211				10. SPONSOR/MONITOR'S ACRONYM(S) ARO	
				11. SPONSOR/MONITOR'S REPORT NUMBER(S) 56039-MS.33	
12. DISTRIBUTION AVAILABILITY STATEMENT Approved for public release; distribution is unlimited.					
13. SUPPLEMENTARY NOTES The views, opinions and/or findings contained in this report are those of the author(s) and should not be construed as an official Department of the Army position, policy or decision, unless so designated by other documentation.					
14. ABSTRACT Single resonance chemical remote sensing, such as Fourier-transform infrared spectroscopy, has limited recognition specificity because of atmospheric pressure broadening. Active interrogation techniques promise much greater chemical recognition that can overcome the limits imposed by atmospheric pressure broadening. Here we introduce infrared - terahertz (IR/THz) double resonance spectroscopy as an active means of chemical remote sensing that retains recognition specificity through rare, molecule-unique coincidences between IR molecular absorption and a					
15. SUBJECT TERMS Submillimeter, Terahertz, Infrared, Chemical sensor					
16. SECURITY CLASSIFICATION OF:			17. LIMITATION OF ABSTRACT UU	15. NUMBER OF PAGES	19a. NAME OF RESPONSIBLE PERSON Frank De Lucia
a. REPORT UU	b. ABSTRACT UU	c. THIS PAGE UU			19b. TELEPHONE NUMBER 614-688-4774

Report Title

Infrared/Terahertz Double Resonance for Chemical Remote Sensing: Signatures and Performance Predictions

ABSTRACT

Single resonance chemical remote sensing, such as Fourier-transform infrared spectroscopy, has limited recognition specificity because of atmospheric pressure broadening. Active interrogation techniques promise much greater chemical recognition that can overcome the limits imposed by atmospheric pressure broadening. Here we introduce infrared - terahertz (IR/THz) double resonance spectroscopy as an active means of chemical remote sensing that retains recognition specificity through rare, molecule-unique coincidences between IR molecular absorption and a line-tunable CO₂ excitation laser. The laser-induced double resonance is observed as a modulated THz spectrum monitored by a THz transceiver. As an example, our analysis indicates that a 1 ppm cloud of CH₃F 100 m thick can be detected at distances up to 1 km using this technique.

Conference Name: Terahertz Physics, Devices, and Systems IV: Advanced Applications in Industry and Defense

Conference Date:

Infrared/Terahertz Double Resonance for Chemical Remote Sensing: Signatures and Performance Predictions

Dane J. Phillips^{1,4}, Elizabeth A. Tanner¹, Henry O. Everitt²
Ivan R. Medvedev³, Christopher F. Neese³, Jennifer Holt³, Frank C. De Lucia³

¹ Kratos Defense – Digital Fusion, ² AMRDEC, ³ Ohio State University, ⁴ University of Alabama in Huntsville

ABSTRACT

Single resonance chemical remote sensing, such as Fourier-transform infrared spectroscopy, has limited recognition specificity because of atmospheric pressure broadening. Active interrogation techniques promise much greater chemical recognition that can overcome the limits imposed by atmospheric pressure broadening. Here we introduce infrared – terahertz (IR/THz) double resonance spectroscopy as an active means of chemical remote sensing that retains recognition specificity through rare, molecule-unique coincidences between IR molecular absorption and a line-tunable CO₂ excitation laser. The laser-induced double resonance is observed as a modulated THz spectrum monitored by a THz transceiver. As an example, our analysis indicates that a 1 ppm cloud of CH₃F 100 m thick can be detected at distances up to 1 km using this technique.

Keywords: Infrared, Terahertz, Spectroscopy, Remote Sensing,

1. INTRODUCTION

Double resonance (DR) spectroscopy is a form of wavelength non-degenerate pump-probe spectroscopic analysis.^[1] For molecular DR spectroscopy, pulsed infrared (IR) radiation excites gas phase molecules, creating a non-equilibrium distribution of population in quantized rotational (and vibrational) states that may be probed by terahertz (THz) radiation. Because the spacing between rotational energy levels ($\sim 1\text{ cm}^{-1}$) is much less than kT (200 cm^{-1} at 300K) while the energies of excited vibrational levels are typically several kT above the ground state, only the rotational manifold in the ground vibrational state will be heavily populated. When IR pump radiation is tuned to coincide with a specific ro-vibrational molecular transition, the pump excites molecules from one of the heavily populated rotational states in the ground vibrational level to one of the sparsely populated rotational states in an excited vibrational level. The dynamical evolution of the non-equilibrium population distributions in both rotational manifolds can be probed with terahertz radiation tuned to coincide with one of the pure rotational transitions in the respective manifold. The strongest DR signals will occur for those rotational transitions containing one level directly affected by the IR pump, and it is these molecule-unique signals that present an opportunity for trace gas remote sensing.

In order to examine the potential of this technique for remote sensing at atmospheric pressures, we will quantitatively compare the expected strength of these DR signals with various natural and system noise sources to estimate the detectable signal to noise ratio (SNR) for various operational scenarios. This manuscript will examine the gas methyl fluoride (CH₃F) because it has been extensively characterized at low pressures in order to demonstrate how DR spectroscopy can overcome the limitations imposed by atmospheric pressure broadening.^[2,3,4] An introduction to low pressure spectroscopic techniques will be followed by estimates of THz DR signatures and their detectability in a representative operational scenario.

2. SINGLE RESONANCE SPECTROSCOPY

Low-pressure ($<100\text{ mTorr}$) rotational spectroscopy provides an exquisitely precise technique for molecular recognition. The spectra, which can be routinely measured with an accuracy of $1:10^7$, depend sensitively on the shape (i.e. moments of inertia and atomic masses) of the molecule.^[5,6] For example, a typical low-pressure rotational spectrum of the prolate symmetric top molecule methyl fluoride (¹²CH₃F) is depicted in Figure 1.

¹ Correspondence: Ph.: (256)955-6081; E-mail: Dane.Phillips@KratosDefense.com

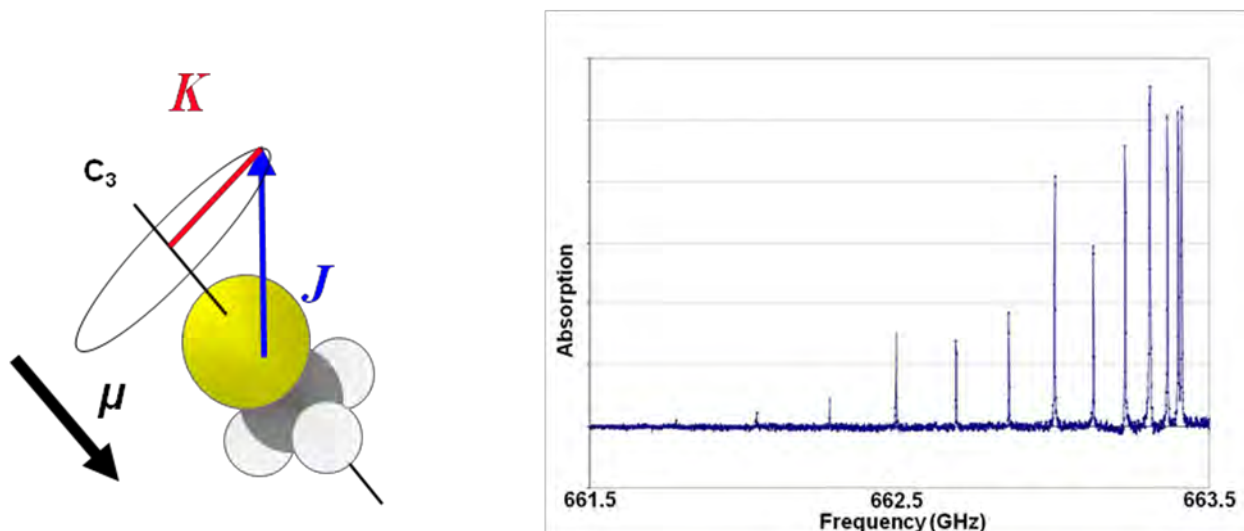


Figure 1: (Left) $^{12}\text{CH}_3\text{F}$ molecule. (Right) $^{12}\text{CH}_3\text{F}$ ground vibrational state, $J = 12 \rightarrow 13$, $K = 0, 1, 2, \dots, 12$ rotational spectrum is shown.

For comparison, the spectrum of the isotopic isomer $^{13}\text{CH}_3\text{F}$ (1% isotopic abundance) occurs at 645 GHz, well separated from the spectrum of $^{12}\text{CH}_3\text{F}$.^[7] The lines in Figure 1 are resolvable because they were obtained at low pressure (10 mTorr) where linewidths are < 1 MHz; however, at atmospheric pressure (760 Torr) specificity is lost because atmospheric pressure broadening produces linewidths of ~ 5 GHz.^[8]

Although not as precise as THz rotational spectroscopy, IR ro-vibrational spectroscopy is widely used for molecular recognition because of the availability of IR spectrometers and the transparency of the atmosphere in the well-known IR windows.^[9] The IR spectrum, which can be routinely measured with an accuracy of $1:10^5$, depends on the type of bond that is vibrating.^[9] For example, the infrared spectrum of the C-F stretch mode in $^{12}\text{CH}_3\text{F}$ is depicted in Figure 2.

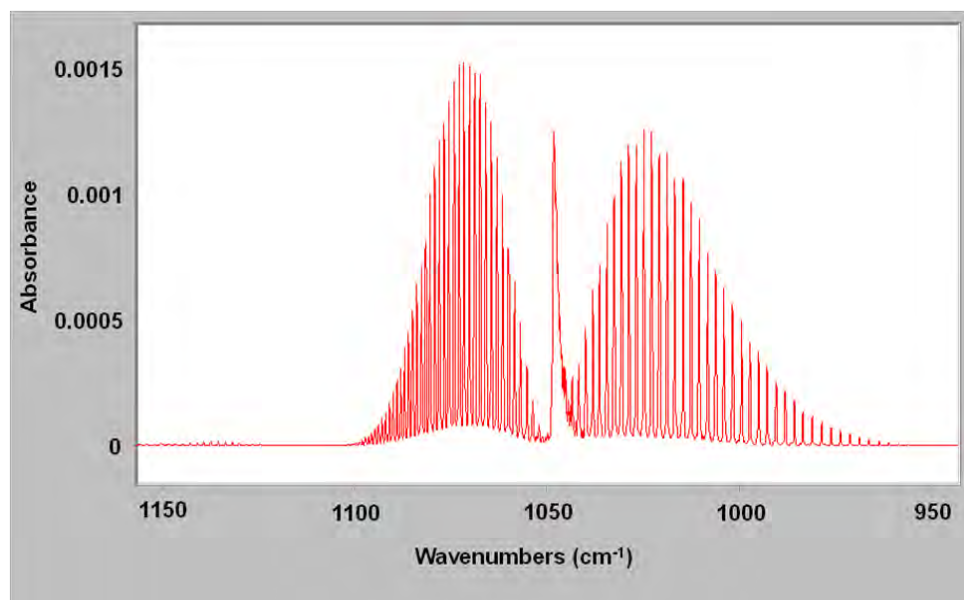


Figure 2: Fourier transform IR spectra of C-F stretch ($V_3 = 1$ level) in $^{12}\text{CH}_3\text{F}$.^[10,11]

Ro-vibrational transitions occur in three distinct types, determined by whether the rotational state changed by $\Delta J = -1, 0$, or 1 .^[9] These are called P-branch, Q-branch, and R-branch transitions, respectively, and are distinguishable as three separate bands from right to left in Figure 2. IR transitions are labeled by the ground rotational state

involved and the type of IR transition, e.g. P(J) for CO₂ or Q(J,K) for symmetric top molecules. Note that Q-branch transitions are not as well resolved as the P- and R-branch transitions.

3. DOUBLE RESONANCE SPECTROSCOPY

Unlike traditional single resonance spectroscopy, which measures the absorption of a transition based on the equilibrium population difference between the upper and lower states, DR spectroscopy measures the change in the population difference induced by the pump. The variation in absorption of a rotational transition can be monitored by measuring the change in coincident terahertz radiation transmitted through the molecular sample. If the pump excitation is strong enough, a rotational population inversion can be induced. This is the basis for low pressure optically pumped far-infrared (OPFIR) lasers.^[12]

OPFIR lasers illustrate the importance of a frequency coincidence between the pump (a CO₂ laser) and a molecular ro-vibrational transition. Although a typical molecule will have thousands of ro-vibrational transitions, it is rare if any of those transitions coincide with any line from a CO₂ laser. For these coincidences to occur, two criteria must be met. First, there must be a vibrational level within the tuning range of a CO₂ laser: between 850 cm⁻¹ and 1150 cm⁻¹. This criterion becomes easier to meet the heavier and more complex the molecule becomes.^[13] Second, a specific molecular ro-vibrational transition must coincide with a specific CO₂ laser line to within the tuning range of the laser (~ 100 MHz) and the linewidth of the transition (~ 30 MHz at low pressure).

When the IR spectrum for the C-F stretch in ¹²CH₃F (red) overlays the available CO₂ laser lines (green), the possibility of coincidences between the two emerges (Figure 3). Although it appears that there should be many naturally occurring coincidences, there are only two close ones at low pressures: the 9P(20) CO₂ laser line can excite the Q(12,1) or Q(12,2) transitions.^[14] Likewise, only one close coincidence occurs at low pressure for ¹³CH₃F: the 9P(32) CO₂ laser line excites the R(4,3) transition.

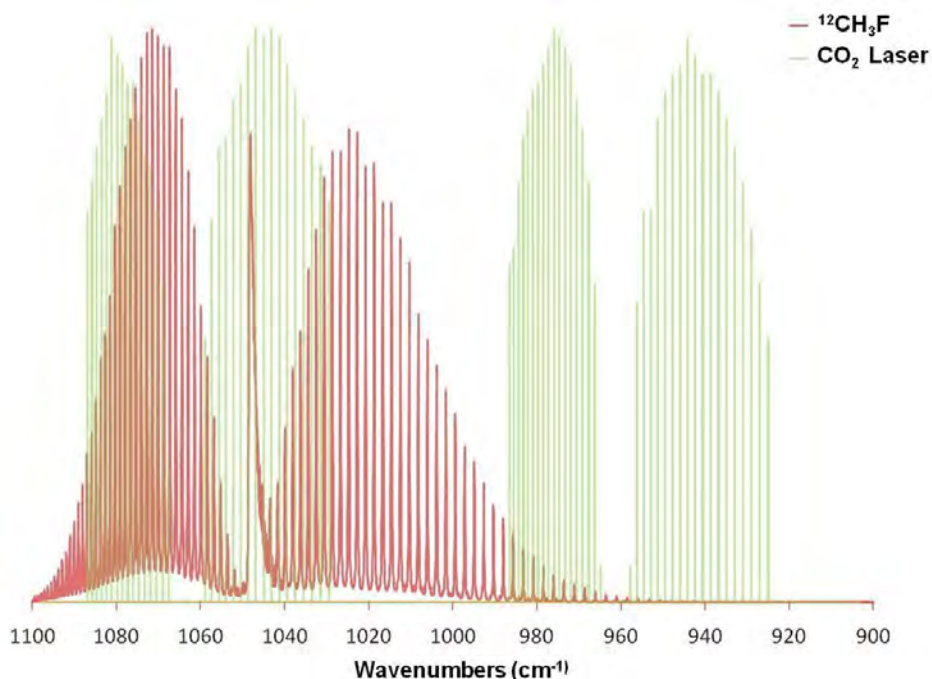


Figure 3: CO₂ laser lines are depicted in green, spectra of ¹²CH₃F is depicted in red.

4. COINCIDENCE MODELING and DOUBLE RESONANCE SIGNATURES

One of the tremendous advantages of performing DR spectroscopy at atmospheric pressure is that the ro-vibrational transitions of the trace gas (e.g. CH₃F) broaden from ~30 MHz to ~ 5 GHz, due to rapid collisions with atmospheric N₂ and O₂, dramatically relaxing the coincidence requirement. To estimate how many more coincidences occur, the ro-vibrational transition frequencies are calculated for all thermally populated rotational states. The frequencies of

these transitions are then compared to the catalog of available CO₂ laser frequencies in order to identify coincidences that are within 5 GHz. In this way, many new coincidences are found, as illustrated in a portion of the ¹²CH₃F Q-branch spectra is depicted in Figure 4.

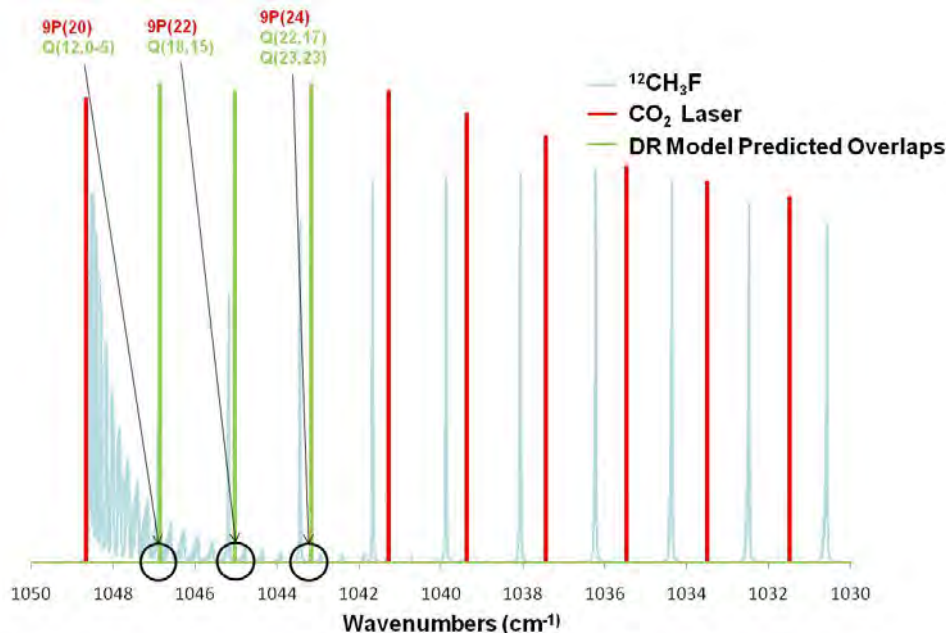


Figure 4: Predicted coincidences (green) between a trace amount of ¹²CH₃F [green, Q(J,K)] in the atmosphere and CO₂ laser lines [red, 9P(J)].

When a ro-vibrational transition is excited by a coincident CO₂ laser line, four rotational transitions are directly connected to the two ro-vibrational levels (Figure 5). Regardless of whether the rotational transition is in the excited or ground vibrational level, the change in absorption of each of the four transitions will be approximately the same: the pump removes the same number of molecules from the “ground state” as it adds to the “excited state”. Of course, the sign of the change will be different, depending on whether the transition is above or below the pumped ro-vibrational level. Two of the rotational transitions will exhibit a pump-induced increase in absorption, and two will exhibit a decrease in absorption or perhaps even emission. The separation between the components is given by the spacing of the rotational levels, which is roughly 2B, where the rotational constant $B \approx 25$ GHz for CH₃F.^[6,15] Note that this 50 GHz of separation allows the DR signature to be well resolved, even at atmospheric pressure where the linewidths are ~5 GHz.

From Figure 5, it is clear that the resulting THz DR signature depends on the type of ro-vibrational transition involved: P-, Q-, or R-branch. P- and R-branch transitions induce opposite DR spectra whose two middle features are of the same sign and nearly overlap. Q-branch transitions, on the other hand, create two doublets of opposite sign whose components nearly overlap. These near-overlaps arise from the difference between the rotational constants in the ground and excited vibrational levels, differences that shrink with increasing molecular mass.^[6] These DR THz spectra are modulated signals that are only detectable when the pulsed laser is exciting the gas and before collisions redistribute the pumped molecules throughout the rotational manifold. The timescale for collisional redistribution is determined by the mean collision time at atmospheric pressure, namely $t = 1/(2 \times \pi \times 2.5 \text{ GHz}) \approx 100$ ps.^[8] Therefore, the DR signal that uniquely identifies the molecule must be excited and measured during this time.

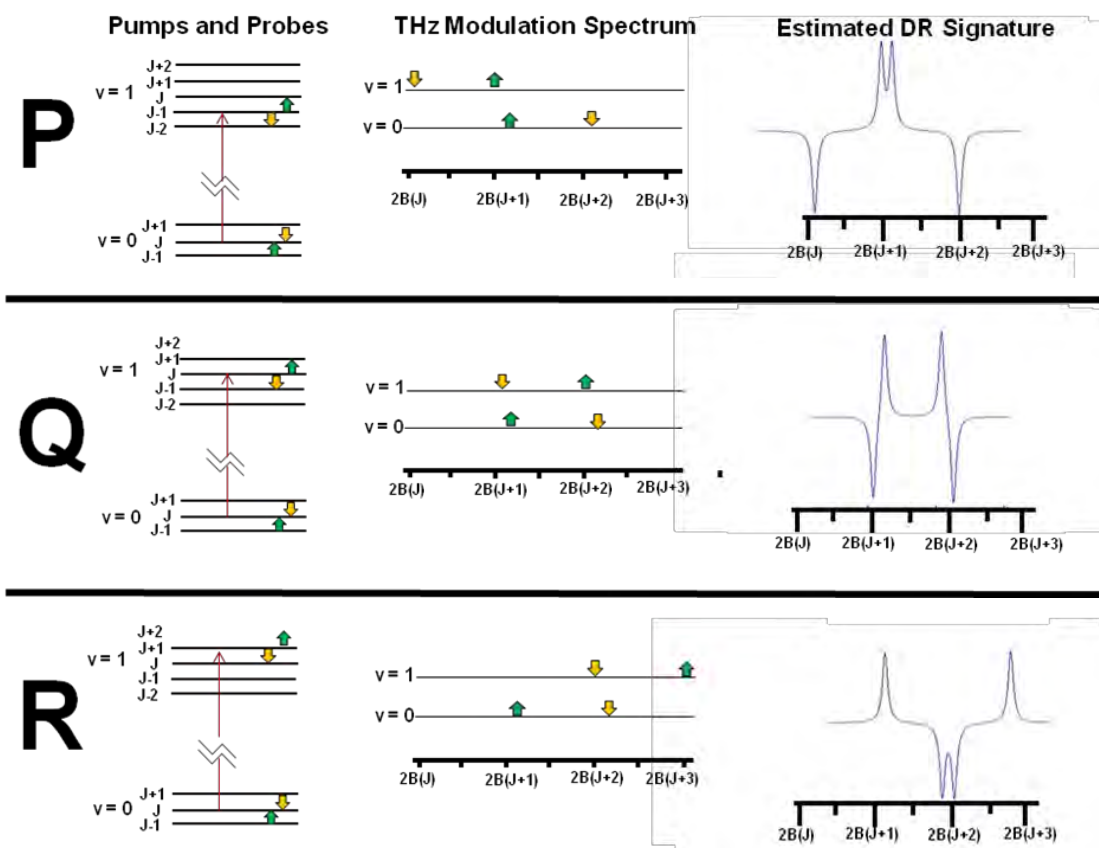


Figure 5. (Left) Notional energy diagram of the ro-vibrational states affected by the pump laser for the three IR transition types (P-, Q-, and R-branch), respectively. (Center) A graphical depiction of the corresponding pump-induced DR signal. (Right) Estimated frequency dependent DR signal for each case.

5. SPECIFICITY

The attributes of rare, molecule-specific pump coincidences and well-resolved DR THz spectra make DR spectroscopy a viable technique for detection of trace gases in the atmosphere in ways exceedingly challenging for more traditional single resonance THz spectroscopy. A two-dimensional specificity matrix can be compiled that indicates the specific combination of IR and THz frequencies that uniquely identify a molecule, even distinguishing isotopic isomers. For example, $^{12}\text{CH}_3\text{F}$ is excited by the 9P(20) line to produce Q-branch DR THz signatures with features at 604.3, 612.4, 654.6 and 663.4 GHz.^[7] $^{13}\text{CH}_3\text{F}$ is excited by the 9P(32) line to produce R-branch DR THz signatures with features at 198.8, 248.6, 245.4, and 294.4 GHz.^[16] This is an enormous difference for two molecules that have identical structures and only differ in mass by 1 amu.

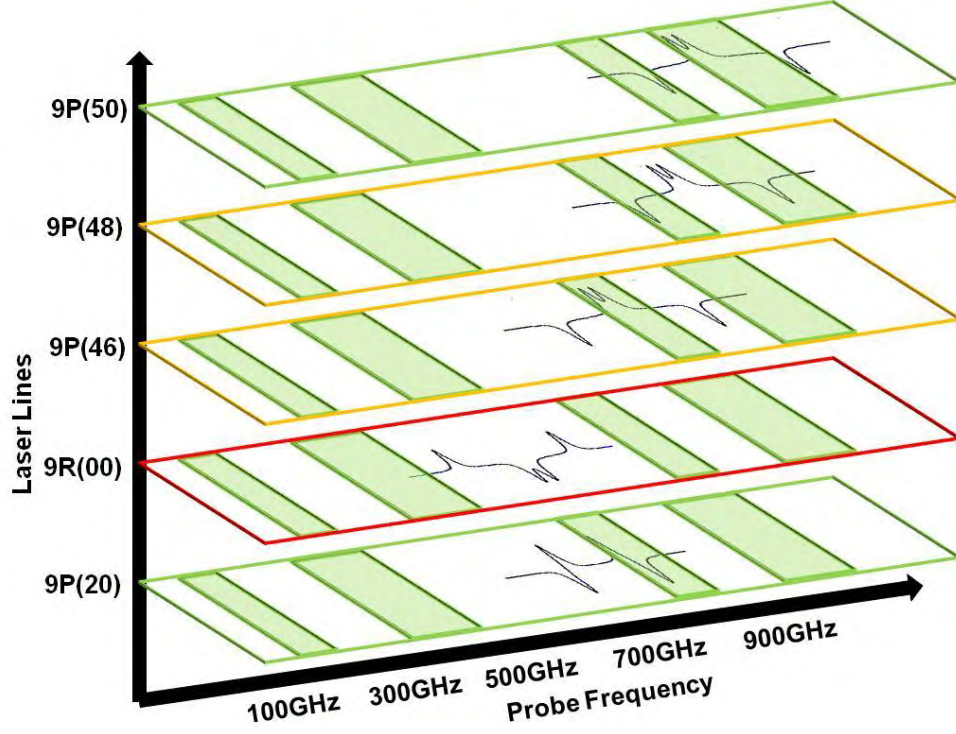


Figure 6: The 2D specificity matrix for $^{12}\text{CH}_3\text{F}$ double resonance remote sensing. The most practical DR spectra for remote sensing are highlighted in green, the least in red.

As the pressure increases, the number of coincidences increases, so that the most convenient combination of pump (IR) and probe (THz) frequencies may be selected. Figure 6 graphically illustrates the specificity matrix of DR signatures for each combination of laser line and THz frequency for $^{12}\text{CH}_3\text{F}$. New coincidences that are predicted to occur at atmospheric pressure are presented above the well-known low pressure coincidence induced by the 9P(20) line. The strength of the DR THz signatures depends strongly on IR absorption strengths, laser line power, atmospheric absorption, and THz source availability. The potential utility of each coincidence is ascertained next.

6. DOUBLE RESONANCE ABSORPTION STRENGTH

To estimate the strength of the pump-induced DR THz signature, consider first the single resonance, frequency-integrated THz absorption coefficient α_{ij} for any of the four transitions involved:

$$\alpha_{ij} = D \frac{8\pi^3 \nu_{ij}^r}{3hc} |\mu_{ij}^r|^2 (n_i - n_j), \quad (1)$$

where i and j are adjacent rotational states in the same vibrational level, ν_{ij}^r and $(n_i - n_j)$ are the (THz) rotational transition frequency and equilibrium population difference between them, and μ_{ij}^r is the dipole matrix element for that rotational transition.^[8] In order to calculate the peak absorption at a given frequency, the integrated absorption coefficient must be multiplied by an area-normalized Lorentzian lineshape function, $S(\nu, \nu_0)$, since the transition is pressure broadened at atmospheric pressure.

Under thermal equilibrium conditions, n_i and n_j are determined though Boltzmann distributions and are dependent upon the total number of molecules present in the molecular gas in a given volume, $n_0 = P/RT$, where P is the partial pressure and T is the temperature of the trace gas. For a trace amount of target molecular gas in an atmosphere the peak absorption is reduced by pressure broadening by a dilution factor, D , which is simply the ratio of the partial

pressure of the gas to atmospheric pressure. For example, the peak absorption for 1 ppm of CH₃F is reduced by $D = 10^{-6}$ over the peak absorption of pure CH₃F of the same (partial) pressure.

Turning now to calculate the DR-induced change in absorption, assume that the pump pulse is comparable to the atmospheric collision time so that there is no collisional thermalization of excited molecules. The pump rate R_{ij} of a particular ro-vibrational transition $i \rightarrow j$ by the CO₂ laser with power p per pulse and beam radius r is given by

$$R_{ij} = \frac{8\pi^2}{3h^2 c} \frac{p}{r^2} |\mu_{ij}^v|^2 S(\nu_p, \nu_o^v) \quad (2)$$

where ν_o^v and μ_{ij}^v are the frequency and ro-vibrational matrix element connecting the ground and excited vibrational state, and the pressure-broadened (Lorentzian), area-normalized line shape function $S(\nu_p, \nu_o^v)$ is included to account for the reduced pumping efficiency when $\nu_p \neq \nu_o^v$.^[17,18,8]

From equation 2 it is evident that as the CO₂ pump irradiance ($p/\pi r^2$) increases, the number of molecules that can be moved per second from the ground vibrational state to the excited vibrational state increases. The number of molecules excited by the pump n_p is then simply the product of R_{ij} , the laser pulse width τ , and the number of molecules in ground rotational state n_i ,

$$n_p = R_{ij} \tau n_i = R_{ij} \tau f_i n_o, \quad (3)$$

where f_i is the fraction of the total molecular population in state i . Since it is assumed that there is no collisional redistribution of population during the brief laser pulse, the modified single resonance THz absorption may be estimated through the change in population of the affected states using (1):

$$\alpha'_{ij} = D \frac{8\pi^3 \nu_{ij}^r}{3hc} |\mu_{ij}^r|^2 (n_i - n_j \mp n_p), \quad (4)$$

where the sign preceding n_p is determined by whether the pump increases (+, green arrows in Fig. 5) or decreases (-, yellow arrows in Fig. 5) the absorption of the rotational transition in question.

Consider the specific case of ¹²CH₃F in which the CO₂ laser excites the Q(12,2) ro-vibrational transition. For the $J = 12 \rightarrow 13$ transition in the ground vibrational level, the pump removes n_p molecules from the equilibrium population n_{12} , so the resulting α'_{12-13} is reduced (Fig. 7(a)) or even inverted if $n_p > n_{12} - n_{13}$ (Fig. 7(b)). Likewise, in the excited vibrational level n_p molecules are added to the $J = 12$ rotational state, causing an increased THz absorption α'_{12-13} , as shown in Figure 7(c).

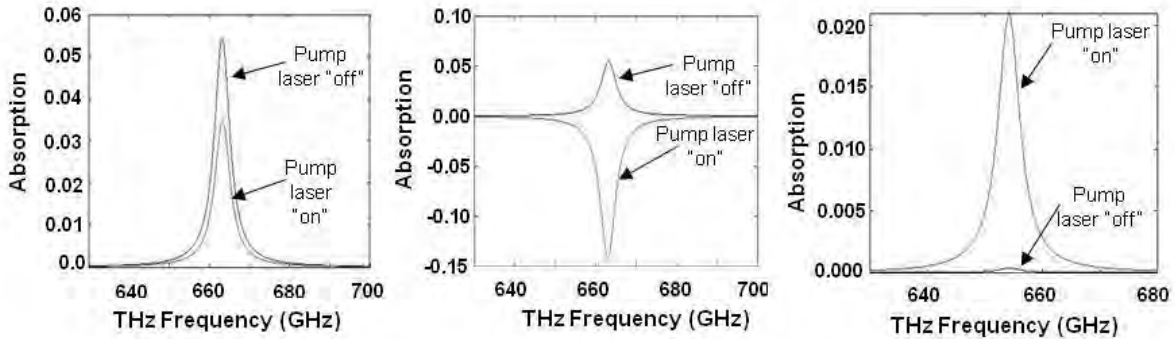


Figure 7: Equilibrium and pumped THz rotational spectra for representative transitions in ¹²CH₃F at a 1ppm concentration, for which the Q(12,2) transition is excited by a 9P(20) CO₂ laser line. (Left) The $J = 12 \rightarrow 13$, $K = 2$ transition in the ground vibrational level for 100 mJ of CO₂ laser power in $r = 100$ cm beam and a 100 ps pulse. (Center) The same transition with 1.0 J of CO₂ laser power. (Right) The same transition and pump parameters as in (Center) but for the $J = 12 \rightarrow 13$, $K = 2$ transition in the excited vibrational level.

The DR THz absorption coefficient, $\Delta\alpha$, is then simply the difference between the equilibrium and pumped absorption coefficients:

$$\Delta\alpha_{ij} = \alpha'_{ij} - \alpha_{ij} = \mp D \frac{8\pi^3 \nu_{ij}^r}{3hc} |\mu_{ij}^r|^2 n_p. \quad (5)$$

This $\Delta\alpha_{ij}$ is what would be measured when remotely sensing trace gases. Notice that $\Delta\alpha_{ij}$ depends linearly on the pump intensity $p/\pi r^2$. More subtly, it depends on the vibrational dipole matrix element μ_{ij}^r , which generally favors P- and R- type ro-vibrational transitions except at low J. It is important to recognize that during the short duration of the pump pulse when thermalizing collisions have not yet occurred, only the four rotational transitions directly connected to the pumped ro-vibrational transition exhibit any THz DR signature. In fact, they have the same $\Delta\alpha_{ij}$: $\Delta\alpha_{12-13,GS} \approx -\Delta\alpha_{11-12,GS} \approx \Delta\alpha_{11-12,ES} \approx -\Delta\alpha_{12-13,ES}$. For all other rotational transitions $\Delta\alpha_{ij} = 0$. When these four components are plotted with the appropriate lineshape function centered on their respective frequencies, the total DR signature for this molecule emerges (Figure 8).

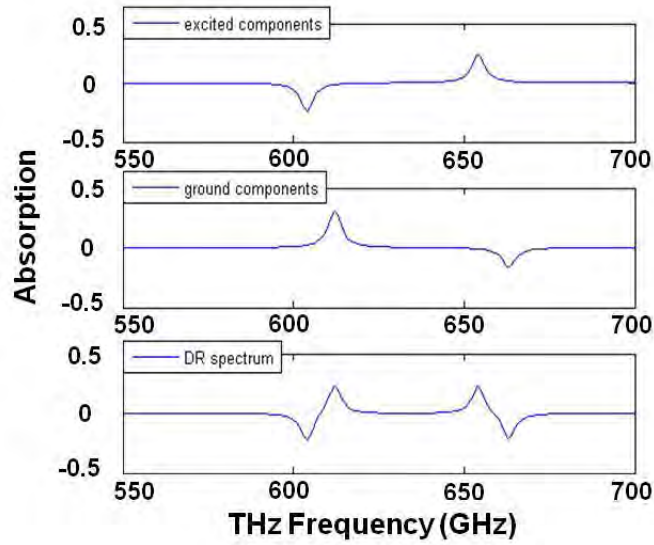


Figure 8: Constituent THz DR spectra in the excited vibrational level (Top) and ground vibrational level (Center), as well as the sum DR signature that would be observed (Bottom).

One final point must be made. Because of the broad lineshapes at atmospheric pressure, the pump laser actually coincides with most if not all $2J+1$ of the K components, making each of the four features in the DR signature the sum of $2J+1$ components. For example, in $^{12}\text{CH}_3\text{F}$, the 9P(20) laser line is actually coincident with ten of the Q(12,K) ro-vibrational transitions ($K = 0-9$) at atmospheric pressure. The DR signatures for each of the constituent K components, and the summed DR signature, are shown in Figure 9.

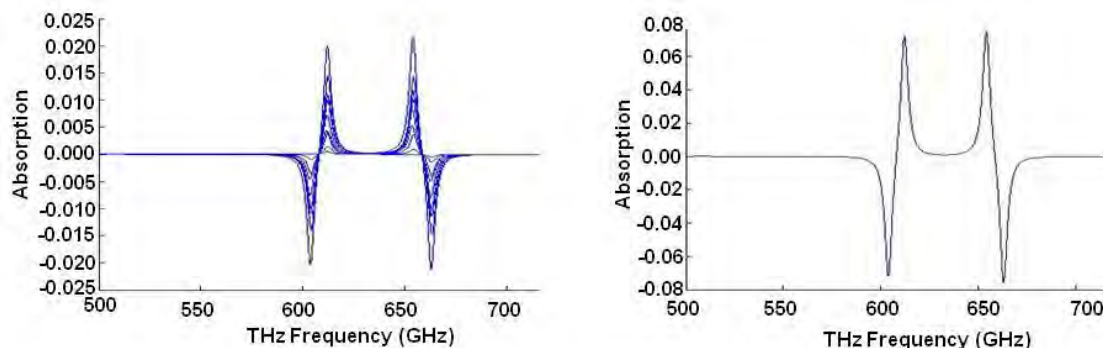


Figure 9: (Left) The individual DR signals from each of the ten K components of excited Q(12,K) transition contributing to the summed $^{12}\text{CH}_3\text{F}$ DR signature (Right). Note the change in vertical scale on the right.

7. DOUBLE RESONANCE REMOTE SENSING

Now that the procedure to estimate THz DR signatures has been described, we may use this calculation to illustrate how double resonance spectroscopy may be used for remote sensing of trace gases^[19]. Suppose the objective was to detect a 100 m thick cloud of 1 ppm methyl fluoride at a distance of 1 km. Assume the IR pump beam and THz probe beam will be configured so that they completely overlap, travel in a horizontal path through cloud, then reflect back to the THz transceiver from a naturally occurring or cooperative background reflector. For long-term monitoring, it is acceptable to use a cooperative retroreflective material, such as copper with a reflectivity of 99%, oriented normal to the transceiver with a size that is at least as large as the diffracted beam at 1km.

Atmospheric attenuation of THz radiation presents a severe restriction on the applicability of this technique. THz DR signatures are only measurable within one of the four atmospheric “windows” identified in Figure 10, whose transparency depends sensitively on the water vapor content of the atmosphere. The ambient atmospheric attenuation, as well as the single resonance THz absorption by the trace gas cloud (equation 1), must be calculated. For the former, we used the clean air Millimeter-wave Propagation Model (MPM) developed by Liebe.^[20] Contributions from molecular oxygen and water are included in the MPM calculations along with the non-resonant dry air spectrum and the water vapor continuum. For the $^{12}\text{CH}_3\text{F}$ THz DR signature occurring at 663 GHz, double pass atmospheric attenuation is 20 dB/km for a 25°F dew point, barely measurable, while it is an unmeasurable 162 dB/km for a 75 °F dew point. Luckily, the relaxed coincidence requirement made possible by atmospheric pressure broadening increases the probability that a given molecule will have a THz DR signature in one of the lower frequency, higher transparency windows.

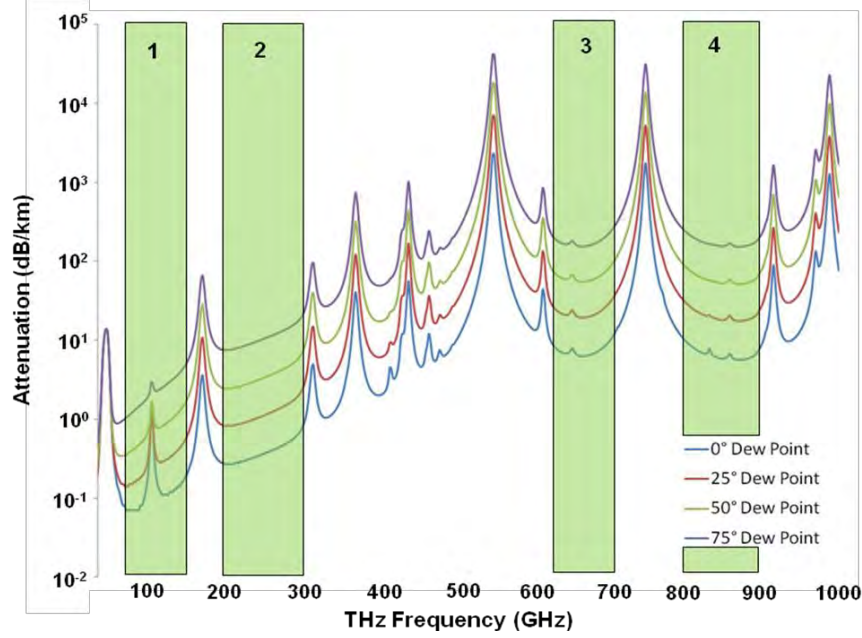


Figure 10: Calculations of atmospheric attenuation of THz propagation for selected dew points. Four atmospheric windows amenable for DR spectroscopy are indicated.

By combining the DR signature calculations and the MPM-based THz propagation models, the scenario-dependent DR signal strength received at the THz transceiver may be estimated as a function of IR pump power and THz transmitter power. For these calculations assume that a mode-locked CO₂ TEA laser provides ten 100 ps, 1 J micropulses per macropulse with a 10 Hz macropulse repetition rate and that a continuous wave THz source emits 100 μ W. The frequency dependent DR spectra generated based on these parameters for ¹²CH₃F is shown in Figure 9.

To ascertain whether or not this DR signal is detectable, an estimate of the system noise must be made. Two otherwise insidious noise sources that plague other remote sensing techniques – blackbody radiation and atmospheric fluctuations – are negligible for this technique, the former because there is virtually no blackbody radiation in the narrow bandpass of the THz heterodyne receiver, the latter because atmospheric fluctuations are frozen on the 100 psec timescale. Of the remaining possible sources of noise, two forms of detector noise dominate: thermal noise and Townes noise.^[6] Because relatively large THz powers will be required, Townes noise will dominate all others:

$$P_N = \sqrt{kT(bB)^{0.5} P_c} \quad (6)$$

where T is the noise temperature of the THz heterodyne receiver, b is the IF bandwidth, and B is the post detection bandwidth. For a THz source power of 100 μ W the received carrier power, after propagation and retroreflection, is $P_c = 4.4 \times 10^{-7}$ W. For a receiver with $T = 1273$ K, $b = 10$ GHz and $B = 10$ GHz, the Townes noise is $\sim 2.8 \times 10^{-8}$ W.

Combining these estimates of the ¹²CH₃F THz DR signal and noise for a 0 °F dew point, the estimated Δa_{ij} produces a laser-induced change in the received THz power of $\sim 1.3 \times 10^{-7}$ W per laser pulse, and for a one second integration time (100 micropulses) the estimated SNR is an easily detectable 46.4. This analysis shows that ¹²CH₃F becomes undetectable at higher dew points because the atmospheric window at 650 GHz closes. However, the isotopic isomer ¹³CH₃F, whose double resonance signature occurs near 250 GHz, remains detectable in spite of its rare, 1% natural abundance even up to the highest relative humidity (Figure 11).^[19] This analysis confirms that it is much more favorable to operate in the lower frequency THz windows because of the reduced sensitivity to water vapor absorption. Our analysis also finds that as molecules become heavier and the B rotational constant decreases, more of the DR THz signatures occur at these lower frequencies. Therefore, if a light molecule like CH₃F can be detected by this technique, heavier molecules are even more likely to be detected.

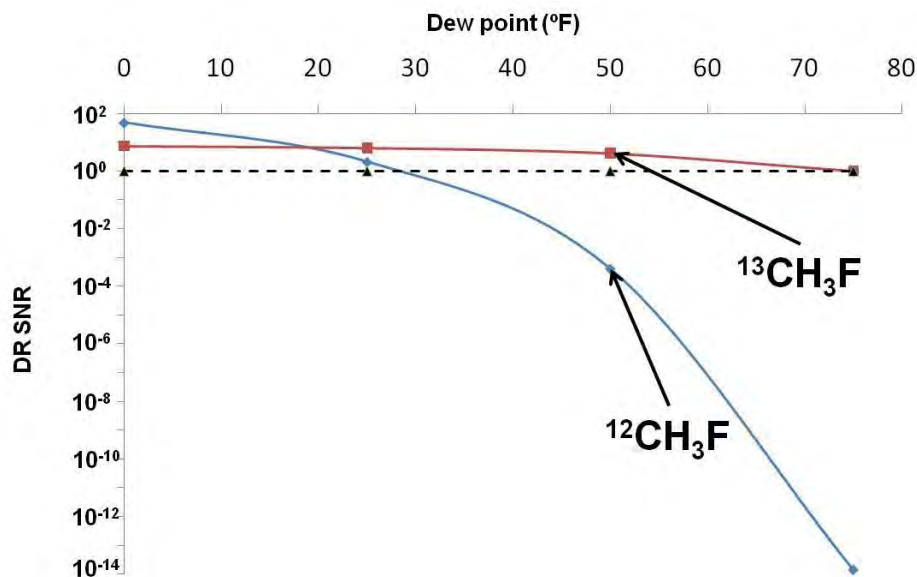


Figure 11: Estimates of the detectability of THz DR signatures as a function of atmospheric water vapor content for the natural abundances of both isotopes of CH_3F , as described in section 7. Calculations are performed at the optimal THz frequency for both isotopes: $^{12}\text{CH}_3\text{F}$ at 663 GHz and $^{13}\text{CH}_3\text{F}$ at 246 GHz. The dashed line indicates an SNR of 1.

8. CONCLUSIONS

The feasibility of IR/THz DR spectroscopy for remote sensing has been demonstrated through an examination of a prototypical molecule, CH_3F in a 1 ppm, 100 m thick cloud at a range of 1 km, detected in plausible scenarios using available or constructible hardware. The sensitivity to pump intensity, ro-vibrational transition type, probe power, atmospheric water vapor content, and location of the THz DR signature within an atmospheric window has been investigated to outline the general applicability of this technique. These insights have revealed certain advantages for working at atmospheric pressure and have indicated a favorable scaling to increasingly heavy and complex molecules.

9. ACKNOWLEDGEMENTS

Partial support for this project has been provided by DTRA, DARPA, and the Army's competitive In-house Laboratory Innovative Research program. Authors DJP, EAT, and HOE would also like to thank Jessica Haack for her support in modeling effort.

10. REFERENCES

- [1] B. Bederson, H. Walker, *Advances in Atomic, Molecular, and Optical Physics* **Vol. 35**, Academic Press, 1995, and references contained therein.
- [2] H. O. Everitt, D. D. Skatrud, F. C. De Lucia, *Appl. Phys. Lett.* **49** (16), 1986.
- [3] H. O. Everitt, F. C. De Lucia, *J. Chem. Phys.* **90** (7), 1989.
- [4] H. O. Everitt, F. C. De Lucia, *J. Chem. Phys.* **92** (11), 1990.
- [5] F. C. De Lucia, *J. Opt. Soc. Am. B.*, **Vol. 21**, No. 7, 2004.
- [6] H. Townes, A. L. Schawlow, *Microwave Spectroscopy*, New York: McGraw-Hill Dover Publications Inc. 1955.
- [7] D. Papousek, et. al., *J. of Mol. Spec.* **196**, 319-323, 1999.

-
- [8] W. Gordy, R. L. Cook, *Microwave Molecular Spectra*, John Wiley & Sons, Inc., 1970.
- [9] J. M. Hollas, *Modern Spectroscopy*, John Wiley & Sons, 2004
- [10] Northwest-Infrared Vapor phase infrared spectral library – Pacific Northwest National Laboratory, Richland WA, <https://secure2.pnl.gov/nsd/nsd.nsf/Welcome>.
- [11] Steven W. Sharpe, et. al, *Applied Spectroscopy*, **Vol. 58**, Num. 12, 2004.
- [12] T. Y. Chang, T. J. Bridges, *Opt. Commun.* **1**, 432-426.
- [13] M. J. Weber, *Handbook of Laser Wavelengths*, CRC Press, 1999.
- [14] Q. Song, R. H. Schwendeman, *J. of Mol. Spec.* **165**, 277-282, 1994.
- [15] D. Papousek, et. al., *J. of Mol. Spec.*, **159**, 33-41, 1991.
- [16] D. Papousek, et. al., *J. of Mol. Spec.*, **192**, 220-227, 1998.
- [17] T. Oka, *Advan. At. Mol. Phys.* **9**, 127 (1973).
- [18] L. Pauling, E. B. Wilson, *Introduction to Quantum Mechanics*, McGraw-Hill, New York, 1935.
- [19] De Lucia, F. C., Petkie, D. T., Everitt, H. O., *IEEE Journal of Quantum Electronics*, **Vol. 45**, 163-170, 2009.
- [20] H. J. Liebe, D. H. Layton, *NTIA Report 87-224*, National Telecommunications and Information Administration, Boulder, CO, 1987.